Answering Visual-Relational Queries in Web-Extracted Knowledge Graphs

Anonymous authors

Abstract

A visual-relational knowledge graph (KG) is a multi-relational graph whose entities are associated with images. We explore novel machine learning approaches for answering visual-relational queries in web-extracted knowledge graphs. To this end, we have created ImageGraph, a KG with 1,330 relation types, 14,870 entities, and 829,931 images crawled from the web. With visual-relational KGs such as ImageGraph one can introduce novel probabilistic query types in which images are treated as first-class citizens. Both the prediction of relations between unseen images as well as multi-relational image retrieval can be expressed with specific families of visual-relational queries. We introduce novel combinations of convolutional networks and knowledge graph embedding methods to answer such queries. We also explore a zero-shot learning scenario where an image of an entirely new entity is linked with multiple relations to entities of an existing KG. The resulting multi-relational grounding of unseen entity images into a knowledge graph serves as a semantic entity representation. We conduct experiments to demonstrate that the proposed methods can answer these visual-relational queries efficiently and accurately.

1. Introduction

Numerous applications can be modeled with a knowledge graph representing entities with nodes, object attributes with node attributes, and relationships between entities by directed typed edges. For instance, a product recommendation system can be represented as a knowledge graph where nodes represent customers and products and where typed edges represent customer reviews and purchasing events. In the medical domain, there are several knowledge graphs that model diseases, symptoms, drugs, genes, and their interactions (cf. [Ashburner et al., 2000, Wishart et al., 2008]). Increasingly, entities in these knowledge graphs are associated with visual data. For instance, in the online retail domain, there are product and advertising images and in the medical domain, there are patient-associated imaging data sets (MRIs, CTs, and so on). In addition, visual data is a large part of social networks and, in general, the world wide web.

[1]Project URL: anonymized for double-blind review

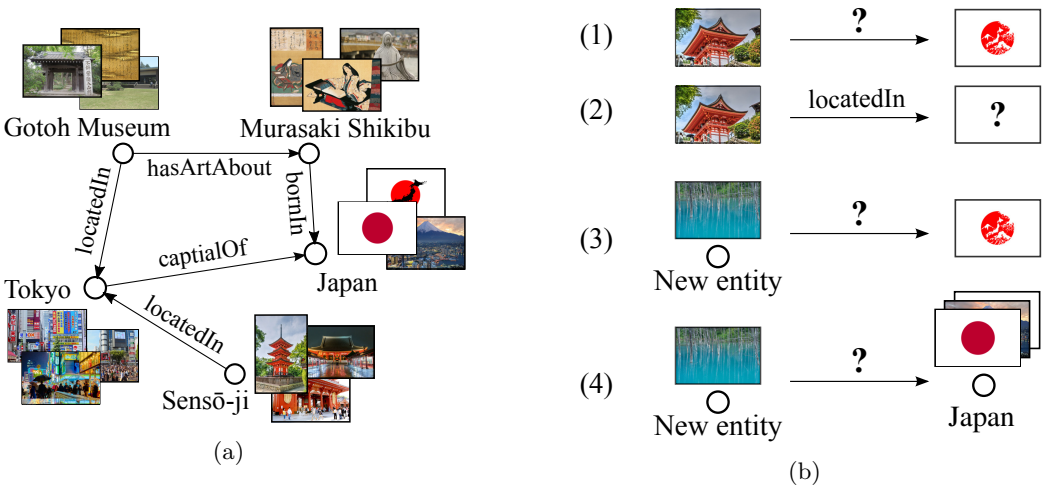

Figure 1: (a) a small part of a visual-relational knowledge graph and a set of query types; and (b) some visual-relational query types;

Knowledge graphs facilitate the integration, organization, and retrieval of structured data and support various forms of search applications. In recent years KGs have been playing an increasingly crucial role in fields such as question answering [Das et al., 2017], language modeling [Ahn et al., 2016], and text generation [Serban et al., 2016]. Even though there is a large body of work on constructing and maintaining KGs, the setting of visual-relational KGs, where entities are associated with visual data, has not received much attention. A visual-relational KG represents entities, relations between these entities, and a large number of images associated with the entities (see Figure 1a for an example). While ImageNet [Deng et al., 2009] and the VisualGenome [Krishna et al., 2016] datasets are based on KGs such as WordNet they are predominantly used as either an object classification data set as in the case of ImageNet or to facilitate scene understanding in a single image. With this work, we address the problem of reasoning about visual concepts across a large set of images organized in a knowledge graph. We want to explore to what extent web-extracted visual data can be used to enrich existing KGs so as to facilitate complex visual search applications going beyond basic image retrieval.

The core idea of our work is to treat images as first-class citizens both in KGs and visual-relational queries. The main objective of our work is to understand to what extent visual data associated with entities of a KG can be used in conjunction with deep learning methods to answer these visual-relational queries. Allowing images to be arguments of queries facilitates numerous novel query types. In Figure 1b we list some of the query types we address in this paper. In order to answer these queries, we built on KG embedding methods as well as deep representation learning approaches for visual data. This allows us to answer these visual queries both accurately and efficiently.

There are numerous application domains that could benefit from query answering in visual KGs. For instance, in online retail, visual representations of novel products could be leveraged for zero-shot product recommendations. Crucially, instead of only being able to retrieve

Table 1: Statistics of the knowledge graphs used in this paper.

	Entities	Relations	Triples			Images		
	$\lvert\mathcal{E}\rvert$	$\lvert\mathcal{R}\rvert$	Train	Valid	Test	Train	Valid	Test
ImageNet [Deng et al., 2009]	21,841	18	-			14,197,122		
VisualGenome [Krishna et al., 2016]	75,729	40,480	1,531,448			108,077		
FB15k [Bordes et al., 2013]	14,951	1,345	483,142	50,000	59,071	0	0	0
ImageGraph	14,870	1,330	460,406	47,533	56,071	411,306	201,832	216,793

Figure 2: Image samples for some entities of ImageGraph.

similar products, a visual-relational KG would support the prediction of product attributes and more specifically what attributes customers might be interested in. For instance, in the fashion industry visual attributes are crucial for product recommendations [Liu et al., 2016, Veit et al., 2015]. Being able to ground novel visual concepts into an existing KG with attributes and various relation types is a reasonable approach to zero-shot learning.

We make the following contributions. First, we introduce ImageGraph, a visual-relational web-extracted KG with 1,330 relations where 829,931 images are associated with 14,870 different entities. Second, we introduce a new set of visual-relational query types. Third, we propose a novel set of neural architectures and objectives that we use for answering these novel query types. These query types generalize image retrieval and link prediction queries. This is the first time that deep CNNs and KG embedding learning objectives are combined into a joint model. Fourth, we show that the proposed class of deep neural networks are also successful for zero-shot learning, that is, creating relations between entirely unseen entities and the KG using only visual data at query time.

2. Related Work

We discuss the relation of our contributions to previous work with an emphasis on relational learning, image retrieval, object detection, scene understanding, existing data sets, and zero-shot learning.

Relational Learning

There has been a flurry of approaches tailored to specific problems such as link prediction in multi-relational graphs. Examples are knowledge base factorization and embedding approaches [Bordes et al., 2013, Nickel et al., 2011, Guu et al., 2015] and random-walk based ML models [Lao et al., 2011, Gardner and Mitchell, 2015]. More recently, the focus has been on integrating additional attribute types such as text [Yahya et al., 2016, C. et al., 2017], temporal graph dynamics [Trivedi et al., 2017], and multiple modalities [Pezeshkpour et al.,

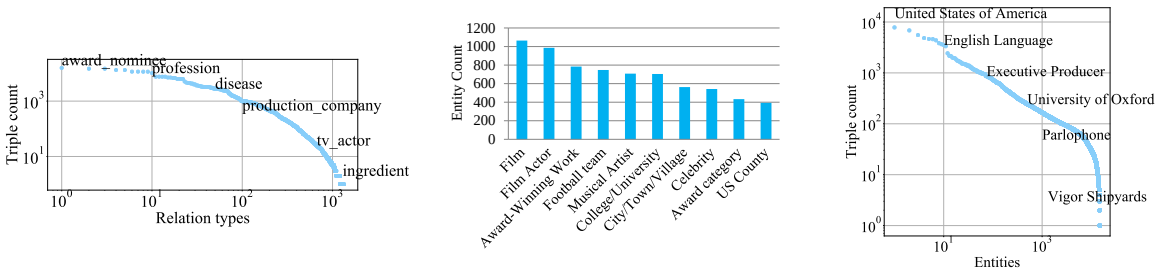

Figure 3: (Left) The distribution of relation types; (center) the 10 most frequent entity types; and (right) the distribution of entities in ImageGraph.

2018]. Another line of research is concerned with extensions of the link prediction problem to multi-hop reasoning [Zhang et al., 2018]. We cannot list all prior link prediction methods here and instead refer the reader to two survey papers [Nickel et al., 2016a, Al Hasan and Zaki, 2011]. Contrary to existing approaches, we address the problem of answering visual-relational queries in knowledge graphs where the entities are associated with web-extracted images. We also address the zero-shot learning scenario, a problem that has not been addressed in the context of link prediction in multi-relational graphs.

Image ranking

Image retrieval is a popular problem and has been addressed by several authors [Wang et al., 2014, Yang et al., 2016, Jiang et al., 2017, Niu et al., 2018, Guy et al., 2018]. In [Yang et al., 2016] a re-ranking of the output of a given search engine by learning a click-based multi-feature similarity is proposed. The authors performed spectral clustering and obtained the final ranked results by computing click-based clusters. In [Guy et al., 2018] the authors fine-tune a DNN to rank photos a user might like to share in social media as well as a mechanism to detect duplicates. In [Niu et al., 2018] a joint user-image embedding is learned to generate a ranking based on user preferences. Contrary to these previous approaches we introduce a set of novel visual query types in a web-extracted KG with images and provide methods to answer these queries efficiently.

Relational and Visual Data

Previous work on combining relational and visual data has focused on object detection [Felzenszwalb et al., 2010, Girshick et al., 2014, Russakovsky et al., 2013, Marino et al., 2017, Li et al., 2017] and scene recognition [Doersch et al., 2013, Pandey and Lazebnik, 2011, Sadeghi and Tappen, 2012, Xiao et al., 2010, Teney et al., 2017] which are required for more complex visual-relational reasoning. Recent years have witnessed a surge in reasoning about human-object, object-object, and object-attribute relationships [Gupta et al., 2009, Farhadi et al., 2009, Malisiewicz and Efros, 2009, Yao and Fei-Fei, 2010, Felzenszwalb et al., 2010, Chen et al., 2013, Izadinia et al., 2014, Zhu et al., 2014]. The VisualGenome project [Krishna et al., 2016] is a knowledge base that integrates language and vision modalities. The project provides a knowledge graph, based on WordNet, which provides annotations of categories, attributes, and relation types for each image. Recent work has used the

dataset to focus on scene understanding in single images. For instance, Lu *et al.* [Lu et al., 2016] proposed a model to detect relation types between objects depicted in an image by inferring sentences such as "man riding bicycle." Veit *et al.* [Veit et al., 2015] propose a siamese CNN to learn a metric representation on pairs of textile products so as to learn which products have similar styles. There is a large body of work on metric learning where the objective is to generate image embeddings such that a pairwise distance-based loss is minimized [Schroff et al., 2015, Bell and Bala, 2015, Oh Song et al., 2016, Sohn, 2016, Wang et al., 2017]. Recent work has extended this idea to directly optimize a clustering quality metric [Song et al., 2017]. In Vincent *et al.* [Vincent et al., 2017] they proposed a mutual embedding space for images and knowledge graphs so the relationships between an image and known entities in a knowledge graph are jointly encoded. Zhou *et al.* [Zhou and Lin, 2016] propose a method based on a bipartite graph that links depictions of meals to its ingredients. Johnson *et al.* [Johnson et al., 2015] propose to use the VisualGenome data to recover images from text queries. ImageGraph is different from these data sets in that the relation types hold between different images and image annotated entities. This defines a novel class of problems where one seeks to answer queries such as "*How are these two images related?*" With this work, we address problems ranging from predicting the relation types for image pairs to multi-relational image retrieval.

Zero-shot Learning

We focus on exploring ways in which KGs can be used to find relationships between visual data of unseen entities, that is, entities not part of the KG during training, and visual data of known KG entities. This is a form of zero-shot learning (ZSL) where the objective is to generalize to novel visual concepts. Generally, ZSL methods (*e.g.* [Romera-Paredes and Torr, 2015, Zhang and Saligrama, 2015]) rely on an underlying embedding space, such as one based on visual attributes, to recognize unseen categories. With this paper, we do not assume the availability of such a common embedding space but we assume the existence of an external visual-relational KG. Similar to our approach, when this explicit knowledge is not encoded in the underlying embedding space, other works rely on finding the similarities through linguistic patterns (*e.g.* [Ba et al., 2015, Lu et al., 2016]), leveraging distributional word representations so as to capture a notion of similarity. These approaches, however, address scene understanding in a single image, *i.e.* these models are able to detect the visual relationships in one given image. Our approach, on the other hand, finds relationships between different images and entities.

3. ImageGraph: A Web-Extracted Visual Knowledge Graph

ImageGraph is a visual-relational KG whose relational structure is based on Freebase [Bollacker et al., 2008] and, more specifically, on FB15k, a subset of FreeBase and a popular benchmark data set [Nickel et al., 2016a]. Since FB15k does not include visual data, we perform the following steps to enrich the KG entities with image data. We implemented a web crawler that is able to parse query results for the image search engines Google Images, Bing Images, and Yahoo Image Search. To minimize the amount of noise due to polysemous entity labels (for example, there are more than 100 Freebase entities with the text label "Springfield") we extracted, for each entity in FB15k, all Wikipedia URIs from the 1.9 billion

Relation type	Example (h, r, t)
Symmetric	`(EmmaThompson,sibling,SophieThompson)` `(SophieThompson,sibling,EmmaThompson)`
Asymmetric	`(Non-profitorganization,company_type,ApacheSoftwareFoundation)` `(Statistics,students_majoring,PhD)`

Others	`(StarWars,film_series,StarWars)`
	`(StarWarsEpisodeI:ThePhantomMenace,film_series,StarWars)`
	`(StarWarsEpisodeII:AttackoftheClones,film_series,StarWars)`

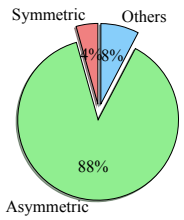

Figure 4: (Left) Example triples for *symmetric*, *asymmetric* and *others* relation types. (Right) Fraction of symmetric, asymmetric, and other relation types among all relation types in ImageGraph.

triple Freebase RDF dump. For instance, for Springfield, Massachusetts, we obtained such URIs as `Springfield_(Massachusetts,United_States)` and `Springfield_(MA)`. These URIs were processed and used as search queries for disambiguation purposes. We used the crawler to download more than 2.4M images (more than 462Gb of data). We removed corrupted, low quality, and duplicate images and we used the 25 top images returned by each of the image search engines whenever there were more than 25 results. The images were scaled to have a maximum height or width of 500 pixels while maintaining their aspect ratio. This resulted in 829,931 images associated with 14,870 different entities (55.8 images per entity). After filtering out triples where either the head or tail entity could not be associated with an image, the visual KG consists of 564,010 triples expressing 1,330 different relation types between 14,870 entities. We provide three sets of triples for training, validation, and testing plus three more image splits also for training, validation and test. Table 1 lists the statistics of the resulting visual KG. Any KG derived from FB15k such as FB15k-237[Toutanova and Chen, 2015] can also be associated with the crawled images. Since providing the images themselves would violate copyright law, we provide the code for the distributed crawler and the list of image URLs crawled for the experiments in this paper[2].

The distribution of relation types is depicted in Figure 3 (left). It plots for each relation type the number of triples it occurs in. Some relation types such as `award_nominee` or `profession` occur quite frequently while others such as `ingredient` have only few instances. 4% of the relation types are symmetric, 88% are asymmetric, and 8% are others (see Table 4 (left)). Table 4 (right) lists specific instances of some relation types. There are 585 distinct entity types such as `Person`, `Athlete`, and `City`. Figure 3 (center) shows the most frequent entity types. Figure 3 (right) visualizes the distribution of entities in the triples of ImageGraph and some example entities.

Table 1 lists some statistics of the ImageGraph KG and other KGs from related work. First, we would like to emphasize the differences between ImageGraph and the Visual Genome project (VG) [Krishna et al., 2016]. With ImageGraph we address the problem of learning a representation for a KG with canonical relation types and not for relation types expressed through text. On a high level, we focus on answering visual-relational queries in a web-extracted KG. This is related to information retrieval except that in our proposed work, images are first-class citizens and we introduce novel and more complex

[2] ImageGraph crawler and URLs: anonymized

query types. In contrast, VGD is focused on modeling relations between objects in images and the relation types are expressed in natural language. Additional differences between ImageGraph and ImageNet are the following. ImageNet is based on WordNet a lexical database where synonymous words from the same lexical category are grouped into synsets. There are 18 relations expressing connections between synsets. In Freebase, on the other hand, there are two orders of magnitudes more relations. In FB15k, the subset we focus on, there are 1,345 relations expressing location of places, positions of basketball players, and gender of entities. Moreover, entities in ImageNet exclusively represent entity types such as `Cats` and `Cars` whereas entities in FB15k are either entity types or instances of entity types such as `Albert Einstein` and `Paris`. This renders the computer vision problems associated with ImageGraph more challenging than those for existing datasets. Moreover, with ImageGraph the focus is on learning relational ML models that incorporate visual data both during learning and at query time.

4. Representation Learning for Visual-Relational Graphs

A knowledge graph (KG) $\mathcal{K}$ is given by a set of triples $\mathbf{T}$, that is, statements of the form $(\mathtt{h}, \mathtt{r}, \mathtt{t})$, where $\mathtt{h}, \mathtt{t} \in \mathcal{E}$ are the head and tail entities, respectively, and $\mathtt{r} \in \mathcal{R}$ is a relation type. Figure 1a depicts a small fragment of a KG with relations between entities and images associated with the entities. Prior work has not included image data and has, therefore, focused on the following two types of queries. First, the query type $(\mathtt{h}, \mathtt{r}?, \mathtt{t})$ asks for the relations between a given pair of head and tail entities. Second, the query types $(\mathtt{h}, \mathtt{r}, \mathtt{t}?)$ and $(\mathtt{h}?, \mathtt{r}, \mathtt{t})$, asks for entities correctly completing the triple. The latter query type is often referred to as knowledge base completion. Here, we focus on queries that involve visual data as query objects, that is, objects that are either contained in the queries, the answers to the queries, or both.

4.1 Visual-Relational Query Answering

When entities are associated with image data, several completely novel query types are possible. Figure 1b lists the query types we focus on in this paper. We refer to images used during training as *seen* and all other images as *unseen*.

(1) Given a pair of *unseen* images for which we do *not* know their KG entities, determine the *unknown* relations between the underlying entities.

(2) Given an *unseen* image, for which we do *not* know the underlying KG entity, and a relation type, determine the *seen* images that complete the query.

(3) Given an *unseen* image of an *entirely new entity* that is not part of the KG, and an *unseen* image for which we do *not* know the underlying KG entity, determine the *unknown* relations between the two underlying entities.

(4) Given an *unseen* image of an *entirely new entity* that is not part of the KG, and a known KG entity, determine the *unknown* relations between the two entities.

For each of these query types, the sought-after relations between the underlying entities have never been observed during training. Query types (3) and (4) are a form of zero-shot

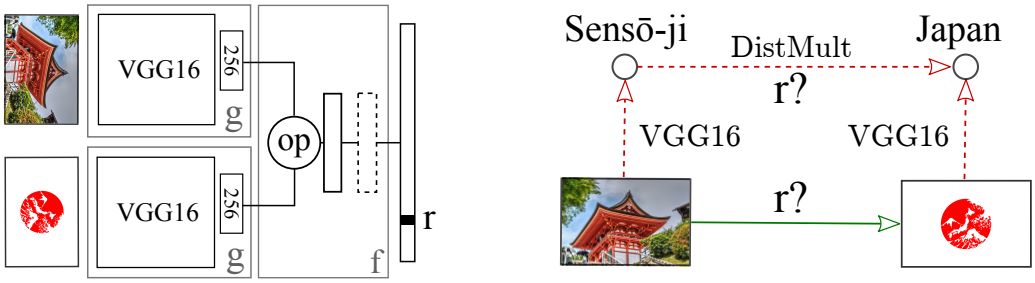

(a) (b)

Figure 5: (a) the proposed architecture for query answering; and (b) an illustration of two possible approaches to visual-relational query answering. One can predict relation types between two images directly (green arrow; our approach) or combine an entity classifier with a KB embedding model for relation prediction (red arrows; baseline `VGG16+DistMult`).

learning since neither the new entity's relationships with other entities nor its images have been observed during training. These considerations illustrate the novel nature of the visual query types. The machine learning models have to be able to learn the relational semantics of the KG and not simply a classifier that assigns images to entities. These query types are also motivated by the fact that for typical KGs the number of entities is orders of magnitude greater than the number of relations.

4.2 Deep Representation Learning for Visual-Relational Query Answering

We first discuss KG completion methods and translate the concepts to query answering in visual-relational KGs. Let $\mathbf{raw}_{\mathtt{i}}$ be the raw feature representation for entity $\mathtt{i} \in \mathcal{E}$ and let f and g be differentiable functions. Most KG completion methods learn an embedding of the entities in a vector space via some *scoring function* that is trained to assign high scores to correct triples and low scores to incorrect triples. Scoring functions have often the form $f_{\mathtt{r}}(\mathbf{e}_{\mathtt{h}}, \mathbf{e}_{\mathtt{t}})$ where $\mathtt{r}$ is a relation type, $\mathbf{e}_{\mathtt{h}}$ and $\mathbf{e}_{\mathtt{t}}$ are d-dimensional vectors (the *embeddings* of the head and tail entities, respectively), and where $\mathbf{e}_{\mathtt{i}} = g(\mathbf{raw}_{\mathtt{i}})$ is an *embedding function* that maps the raw input representation of entities to the embedding space. In the case of KGs without visual data, the raw representation of an entity is simply its one-hot encoding.

Existing KG completion methods use the embedding function $g(\mathbf{raw}_{\mathtt{i}}) = \mathbf{raw}_{\mathtt{i}}^{\intercal}\mathbf{W}$ where $\mathbf{W}$ is a $|\mathcal{E}| \times d$ matrix, and differ only in their scoring function, that is, in the way the embeddings of the head and tail entities are combined with the parameter vector $\boldsymbol{\phi}_{\mathtt{r}}$:

- Difference (TransE[Bordes et al., 2013]): $f_{\mathtt{r}}(\mathbf{e}_{\mathtt{h}}, \mathbf{e}_{\mathtt{t}}) = -||\mathbf{e}_{\mathtt{h}} + \boldsymbol{\phi}_{\mathtt{r}} - \mathbf{e}_{\mathtt{t}}||_2$ where $\boldsymbol{\phi}_{\mathtt{r}}$ is a d-dimensional vector;
- Multiplication (DistMult[Yang et al., 2014]): $f_{\mathtt{r}}(\mathbf{e}_{\mathtt{h}}, \mathbf{e}_{\mathtt{t}}) = (\mathbf{e}_{\mathtt{h}} * \mathbf{e}_{\mathtt{t}}) \cdot \boldsymbol{\phi}_{\mathtt{r}}$ where $*$ is the element-wise product and $\boldsymbol{\phi}_{\mathtt{r}}$ a d-dimensional vector;
- Circular correlation (HoLE[Nickel et al., 2016b]): $f_{\mathtt{r}}(\mathbf{e}_{\mathtt{h}}, \mathbf{e}_{\mathtt{t}}) = (\mathbf{e}_{\mathtt{h}} \star \mathbf{e}_{\mathtt{t}}) \cdot \boldsymbol{\phi}_{\mathtt{r}}$ where $[\mathbf{a} \star \mathbf{b}]_k = \sum_{i=0}^{d-1} \mathbf{a}_i \mathbf{b}_{(i+k) \ \mathtt{mod} \ d}$ and $\boldsymbol{\phi}_{\mathtt{r}}$ a d-dimensional vector; and

- Concatenation: $f_{\mathtt{r}}(\mathbf{e}_{\mathtt{h}}, \mathbf{e}_{\mathtt{t}}) = (\mathbf{e}_{\mathtt{h}} \odot \mathbf{e}_{\mathtt{t}}) \cdot \boldsymbol{\phi}_{\mathbf{r}}$ where $\odot$ is the concatenation operator and $\boldsymbol{\phi}_{\mathbf{r}}$ a $2d$-dimensional vector.

For each of these instances, the matrix $\mathbf{W}$ (storing the entity embeddings) and the vectors $\boldsymbol{\phi}_{\mathtt{r}}$ are learned during training. In general, the parameters are trained such that $f_{\mathtt{r}}(\mathbf{e}_{\mathtt{h}}, \mathbf{e}_{\mathtt{t}})$ is high for true triples and low for triples assumed not to hold in the KG. The training objective is often based on the logistic loss, which has been shown to be superior for most of the composition functions [Trouillon et al., 2016],

$$\min_{\Theta} \sum_{(\mathtt{h},\mathtt{r},\mathtt{t}) \in \mathbf{T}_{\mathtt{pos}}} \log(1 + \exp(-f_{\mathtt{r}}(\mathbf{e}_{\mathtt{h}}, \mathbf{e}_{\mathtt{t}})) + \sum_{(\mathtt{h},\mathtt{r},\mathtt{t}) \in \mathbf{T}_{\mathtt{neg}}} \log(1 + \exp(f_{\mathtt{r}}(\mathbf{e}_{\mathtt{h}}, \mathbf{e}_{\mathtt{t}}))) + \lambda ||\Theta||_2^2, \quad (1)$$

where $\mathbf{T}_{\mathtt{pos}}$ and $\mathbf{T}_{\mathtt{neg}}$ are the set of positive and negative training triples, respectively, Θ are the parameters trained during learning and λ is a regularization hyperparameter. For the above objective, a process for creating corrupted triples $\mathbf{T}_{\mathtt{neg}}$ is required. This often involves sampling a random entity for either the head or tail entity. To answer queries of the types $(\mathtt{h}, \mathtt{r}, \mathtt{t}?)$ and $(\mathtt{h}?, \mathtt{r}, \mathtt{t})$ after training, we form all possible completions of the queries and compute a ranking based on the scores assigned by the trained model to these completions.

For the queries of type $(\mathtt{h}, \mathtt{r}?, \mathtt{t})$ one typically uses the softmax activation in conjunction with the categorical cross-entropy loss, which does not require negative triples

$$\min_{\Theta} \sum_{(\mathtt{h},\mathtt{r},\mathtt{t}) \in \mathbf{T}_{\mathtt{pos}}} -\log \left(\frac{\exp(f_{\mathtt{r}}(\mathbf{e}_{\mathtt{h}}, \mathbf{e}_{\mathtt{t}}))}{\sum_{\mathtt{r} \in \mathcal{R}} \exp(f_{\mathtt{r}}(\mathbf{e}_{\mathtt{h}}, \mathbf{e}_{\mathtt{t}}))} \right) + \lambda ||\Theta||_2^2, \quad (2)$$

where Θ are the parameters trained during learning.

For visual-relational KGs, the input consists of raw image data instead of the one-hot encodings of entities. The approach we propose builds on the ideas and methods developed for KG completion. Instead of having a simple embedding function $\mathtt{g}$ that multiplies the input with a weight matrix, however, we use deep convolutional neural networks to extract meaningful visual features from the input images. For the composition function $\mathtt{f}$ we evaluate the four operations that were used in the KG completion literature: difference, multiplication, concatenation, and circular correlation. Figure 5a depicts the basic architecture we trained for query answering. The weights of the parts of the neural network responsible for embedding the raw image input, denoted by $\mathtt{g}$, are tied. We also experimented with additional hidden layers indicated by the dashed dense layer. The composition operation **op** is either difference, multiplication, concatenation, or circular correlation. To the best of our knowledge, this is the first time that KG embedding learning and deep CNNs have been combined for visual-relationsl query answering.

5. Experiments

We conduct a series of experiments to evaluate the proposed approach. First, we describe the experimental set-up that applies to all experiments. Second, we report and interpret results for the different types of visual-relational queries.

5.1 General Set-up

We used Caffe, a deep learning framework [Jia et al., 2014] for designing, training, and evaluating the proposed models. The embedding function $\mathtt{g}$ is based on the VGG16 model introduced in [Simonyan and Zisserman, 2014]. We pre-trained the VGG16 on the ILSVRC2012 data set derived from ImageNet [Deng et al., 2009] and removed the softmax layer of the original VGG16. We added a 256-dimensional layer after the last dense layer of the VGG16. The output of this layer serves as the embedding of the input images. The reason for reducing the embedding dimensionality from 4096 to 256 is motivated by the objective to obtain an efficient and compact latent representation that is feasible for KGs with billion of entities. For the composition function $\mathtt{f}$, we performed either of the four operations difference, multiplication, concatenation, and circular correlation. We also experimented with an additional hidden layer with ReLu activation. Figure 5a depicts the generic network architecture. The output layer of the architecture has a softmax or sigmoid activation with cross-entropy loss. We initialized the weights of the newly added layers with the Xavier method [Glorot and Bengio, 2010].

We used a batch size of 45 which was the maximal possible fitting into GPU memory. To create the training batches, we sample a random triple uniformly at random from the training triples. For the given triple, we randomly sample one image for the head and one for the tail from the set of training images. We applied SGD with a learning rate of 10^{-5} for the parameters of the VGG16 and a learning rate of 10^{-3} for the remaining parameters. It is crucial to use two different learning rates since the large gradients in the newly added layers would lead to unreasonable changes in the pretrained part of the network. We set the weight decay to 5×10^{-4}. We reduced the learning rate by a factor of 0.1 every 40,000 iterations. Each of the models was trained for 100,000 iterations.

Since the answers to all query types are either rankings of images or rankings of relations, we utilize metrics measuring the quality of rankings. In particular, we report results for hits@1 (hits@10, hits@100) measuring the percentage of times the correct relation was ranked highest (ranked in the top 10, top 100). We also compute the median of the ranks of the correct entities or relations and the Mean Reciprocal Rank (MRR) for entity and relation rankings, respectively, defined as follows:

$$\text{MRR} = \frac{1}{2|\mathbf{T}|} \sum_{(\mathtt{h},\mathtt{r},\mathtt{t}) \in \mathbf{T}} \left(\frac{1}{\mathtt{rank}_{\mathtt{img}(\mathtt{h})}} + \frac{1}{\mathtt{rank}_{\mathtt{img}(\mathtt{t})}} \right) \tag{3}$$

$$\text{MRR} = \frac{1}{|\mathbf{T}|} \sum_{(\mathtt{h},\mathtt{r},\mathtt{t}) \in \mathbf{T}} \frac{1}{\mathtt{rank}_{\mathtt{r}}}, \tag{4}$$

where $\mathbf{T}$ is the set of all test triples, $\mathtt{rank}_{\mathtt{r}}$ is the rank of the correct relation, and $\mathtt{rank}_{\mathtt{img}(\mathtt{h})}$ is the rank of the highest ranked image of entity $\mathtt{h}$. For each query, we remove all triples that are also correct answers to the query from the ranking. All experiments were run on commodity hardware with 128GB RAM, a single 2.8 GHz CPU, and a NVIDIA 1080 Ti.

5.2 Visual Relation Prediction

Given a pair of unseen images we want to determine the relations between their underlying unknown entities. This can be expressed with $(\mathtt{img}_{\mathtt{h}}, \mathtt{r}?, \mathtt{img}_{\mathtt{t}})$. Figure 1b illustrates this

Table 2: Results for the relation prediction problem.

Model	Median	Hits@1	Hits@10	MRR
`VGG16+DistMult`	94	6.0	11.4	0.087
Prob. Baseline	35	3.7	26.5	0.104
DIFF	11	21.1	50.0	0.307
MULT	8	15.5	54.3	0.282
CAT	**6**	**26.7**	**61.0**	**0.378**
DIFF+1HL	8	22.6	55.7	0.333
MULT+1HL	9	14.8	53.4	0.273
CAT+1HL	**6**	25.3	60.0	0.365

query type which we refer to as visual relation prediction. We train the deep architectures using the training and validation triples and images, respectively. For each triple $(\mathtt{h}, \mathtt{r}, \mathtt{t})$ in the training data set, we sample one training image uniformly at random for both the head and the tail entity. We use the architecture depicted in Figure 5a with the softmax activation and the categorical cross-entropy loss. For each test triple, we sample one image uniformly at random from the test images of the head and tail entity, respectively. We then use the pair of images to query the trained deep neural networks. To get a more robust statistical estimate of the evaluation measures, we repeat the above process three times per test triple. Again, none of the test triples and images are seen during training nor are any of the training images used during testing. Computing the answer to one query takes the model 20 ms.

We compare the proposed architectures to two different baselines: one based on entity classification followed by a KB embedding method for relation prediction (`VGG16+DistMult`), and a probabilistic baseline (Prob. Baseline). The entity classification baseline consists of fine-tuning a pretrained VGG16 to classify images into the $14,870$ entities of ImageGraph. To obtain the relation type ranking at test time, we predict the entities for the head and the tail using the VGG16 and then use the KB embedding method DistMult[Yang et al., 2014] to return a ranking of relation types for the given (head, tail) pair. `DistMult` is a KB embedding method that achieves state of the art results for KB completion on FB15k [Kadlec et al., 2017]. Therefore, for this experiment we just substitute the original output layer of the VGG16 pretrained on ImageNet with a new output layer suitable for our problem. To train, we join the train an validation splits, we set the learning rate to 10^{-5} for all the layers and we train following the same strategy that we use in all of our experiments. Once the system is trained, we test the model by classifying the entities of the images in the test set. To train `DistMult`, we sample 500 negatives triples for each positive triple and used an embedding size of 100. Figure 5b illustrates the `VGG16+DistMult` baseline and contrasts it with our proposed approach. The second baseline (probabilistic baseline) computes the probability of each relation type using the set of training and validation triples. The baseline ranks relation types based on these prior probabilities.

Table 2 lists the results for the two baselines and the different proposed architectures. The probabilistic baseline outperforms the `VGG16+DistMult` baseline in 3 of the metrics. This is due to the highly skewed distribution of relation types in the training, validation, and

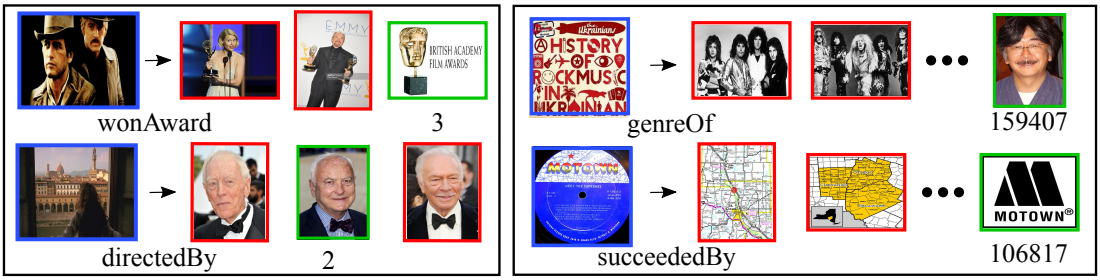

Figure 6: Example queries and qualitative results for the multi-relational image retrieval problem.

Table 3: Results for multi-relational image retrieval.

	Median		Hits@100		MRR	
Model	Head	Tail	Head	Tail	Head	Tail
Baseline	6504	2789	11.9	18.4	**0.065**	**0.115**
DIFF	1301	877	19.6	26.3	0.051	0.094
MULT	1676	1136	16.8	22.9	0.040	0.080
CAT	1022	727	21.4	27.5	0.050	0.087
DIFF+1HL	1644	1141	15.9	21.9	0.045	0.085
MULT+1HL	2004	1397	14.6	20.5	0.034	0.069
CAT+1HL	1323	919	17.8	23.6	0.042	0.080
CAT-SIG	**814**	**540**	**23.2**	**30.1**	0.049	0.082

test triples. A small number of relation types makes up a large fraction of triples. Figure 3 (left) and 3 (right) depicts the plots of the counts of relation types and entities. Moreover, despite DistMult achieving a hits@1 value of 0.46 for the relation prediction problem between entity pairs the baseline `VGG16+DistMult` performs poorly. This is due to the poor entity classification performance of the VGG (accurracy: 0.082, F1: 0.068). In the remainder of the experiments, therefore, we only compare to the probabilistic baseline. In the lower part of Table 2, we lists the results of the experiments. DIFF, MULT, and CAT stand for the different possible composition operations. We omitted the composition operation circular correlation since we were not able to make the corresponding model converge, despite trying several different optimizers and hyperparameter settings. The post-fix 1HL stands for architectures where we added an additional hidden layer with ReLu activation before the softmax. The concatenation operation clearly outperforms the multiplication and difference operations. This is contrary to findings in the KG completion literature where MULT and DIFF outperformed the concatenation operation. The models with the additional hidden layer did not perform better than their shallower counterparts with the exception of the DIFF model. We hypothesize that this is due to difference being the only linear composition operation, benefiting from an additional non-linearity. Each of the proposed models outperforms the baselines.

	Median		Hits@1		Hits@10		MRR	
	H	T	H	T	H	T	H	T
Zero-Shot Query (3)								
Base	34	31	1.9	2.3	18.2	28.7	0.074	0.089
CAT	**8**	**7**	**19.1**	**22.4**	**54.2**	**57.9**	**0.306**	**0.342**
Zero-Shot Query (4)								
Base	9	5	13.0	22.6	52.3	64.8	0.251	0.359
CAT	**5**	**3**	**26.9**	**33.7**	**62.5**	**70.4**	**0.388**	**0.461**

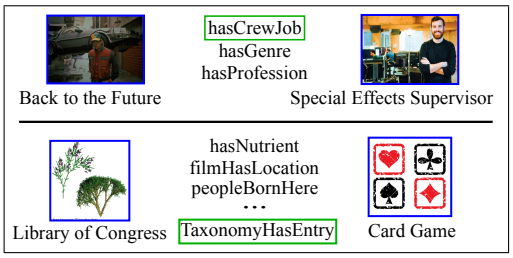

Figure 7: (Left) Results for the zero-shot learning experiments. (Right) Example results for zero-shot learning. For each pair of images the top three relation types (as ranked by the CAT model) are listed. For the pair of images at the top, the first relation type is correct. For the pair of images at the bottom, the correct relation type `TaxonomyHasEntry` is not among the top three relation types.

5.3 Multi-Relational Image Retrieval

Given an unseen image, for which we do not know the underlying KG entity, and a relation type, we want to retrieve existing images that complete the query. If the image for the head entity is given, we return a ranking of images for the tail entity; if the tail entity image is given we return a ranking of images for the head entity. This problem corresponds to query type (2) in Figure 1b. Note that this is equivalent to performing multi-relational metric learning which, to the best of our knowledge, has not been done before. We performed experiments with each of the three composition functions $\mathtt{f}$ and for two different activation/loss functions. First, we used the models trained with the softmax activation and the categorical cross-entropy loss to rank images. Second, we took the models trained with the softmax activation and substituted the softmax activation with a sigmoid activation and the corresponding binary cross-entropy loss. For each training triple $(\mathtt{h}, \mathtt{r}, \mathtt{t})$ we then created two negative triples by sampling once the head and once the tail entity from the set of entities. The negative triples are then used in conjunction with the binary cross-entropy loss of equation 1 to refine the pretrained weights. Directly training a model with the binary cross-entropy loss was not possible since the model did not converge properly. Pretraining with softmax and categorical cross-entropy loss was crucial to make the binary loss work.

During testing, we used the test triples and ranked the images based on the probabilities returned by the respective models. For instance, given the query $(\mathtt{img}_{\mathtt{Sensō\text{-}ji}}, \mathtt{locatedIn}, \mathtt{img}_{\mathtt{t}}?)$, we substituted $\mathtt{img}_{\mathtt{t}}?$ with all training and validation images, one at a time, and ranked the images according to the probabilities returned by the models. We use the rank of the highest ranked image belonging to the true entity (here: `Japan`) to compute the values for the evaluation measures. We repeat the same experiment three times (each time randomly sampling the images) and report average values. Again, we compare the results for the different architectures with a probabilistic baseline. For the baseline, however, we compute a distribution of head and tail entities for each of the relation types. For example, for the relation type `locatedIn` we compute two distributions, one for head and one for tail entities. We used the same measures as in the previous experiment to evaluate the returned image rankings.

Table 3 lists the results of the experiments. As for relation prediction, the best performing models are based on the concatenation operation, followed by the difference and multiplication operations. The architectures with an additional hidden layer do not improve the performance. We also provide the results for the concatenation-based model with softmax activation where we refined the weights using a sigmoid activation and negative sampling as described before. This model is the best performing model. All neural network models are significantly better than the baseline with respect to the median and hits@100. However, the baseline has slightly superior results for the MRR. This is due to the skewed distribution of entities and relations in the KG (see Figure 3 (right) and Figure 3 (left)). This shows once more that the baseline is highly competitive for the given KG. Figure 6 visualizes the answers the CAT-SIG model provided for a set of four example queries. For the two queries on the left, the model performed well and ranked the correct entity in the top 3 (green frame). The examples on the right illustrate queries for which the model returned an inaccurate ranking. To perform query answering in a highly efficient manner, we precomputed and stored all image embeddings once, and only compute the scoring function (involving the composition operation and a dot product with $\boldsymbol{\phi}_{\mathbf{r}}$) at query time. Answering one multi-relational image retrieval query (which would otherwise require 613,138 individual queries, one per possible image) took only 90 ms.

5.4 Zero-Shot Visual Relation Prediction

The last set of experiments addresses the problem of zero-shot learning. For both query types, we are given an new image of an entirely new entity that is not part of the KG. The first query type asks for relations between the given image and an unseen image for which we do not know the underlying KG entity. The second query type asks for the relations between the given image and an existing KG entity. We believe that creating multi-relational links to existing KG entities is a reasonable approach to zero-shot learning since the relations to existing visual concepts and their attributes provide a characterization of the new entity/category.

For the zero-shot experiments, we generated a new set of training, validation, and test triples. We randomly sampled 500 entities that occur as head (tail) in the set of test triples. We then removed all training and validation triples whose head or tail is one of these 1000 entities. Finally, we only kept those test triples with one of the 1000 entities either as head or tail but not both. For query type (4) where we know the target entity, we sample 10 of its images and use the models 10 times to compute a probability. We use the average probabilities to rank the relations. For query type (3) we only use one image sampled randomly. As with previous experiments, we repeated procedure three times and averaged the results. For the baseline, we compute the probabilities of relation in the training and validation set (for query type (3)) and the probabilities of relations conditioned on the target entity (for query type (4)). Again, these are very competitive baselines due to the skewed distribution of relations and entities. Table 7 (left) lists the results of the experiments. The model based on the concatenation operation (CAT) outperforms the baseline and performs surprisingly well. The deep models are able to generalize to unseen images since their performance is comparable to the performance in the relation prediction task (query type (1)) where the entity was part of the KG during training (see Table 2). Figure 7 (right)

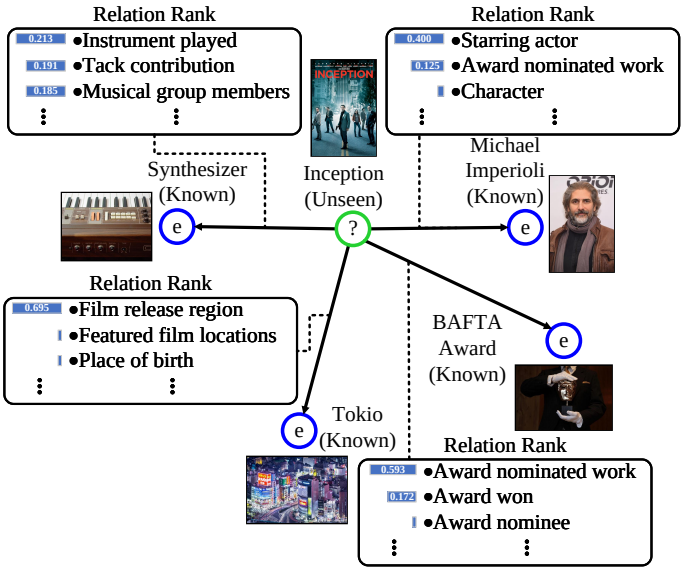

Figure 8: Qualitative example of the zero-shot learning problem. The plot shows the most probable relations that link a sample from an unknown entity (green) with samples of known entities (blue) of the KG.

depicts example queries for the zero-shot query type (3). For the first query example, the CAT model ranked the correct relation type first (indicated by the green bounding box). The second example is more challenging and the correct relation type was not part of the top 10 ranked relation types. Figure 5.4 shows one concrete example of the zero-shot learning problem. In green, visual data from an unknown entity is linked with visual data from KG entities (blue) by ranking the most probable relation types. This problem cannot be addressed with standard relation prediction methods since entities need to be part of the KG during training for these models to work.

6. Conclusion

KGs are at the core of numerous AI applications. Research has focused either on link prediction working only on the relational structure or on scene understanding in a single image. We present a novel visual-relational KG where the entities are enriched with visual data. We proposed several novel query types and introduce neural architectures suitable for probabilistic query answering. We propose a novel approach to zero-shot learning as the problem of visually mapping an image of an entirely new entity to a KG.

References

Sungjin Ahn, Heeyoul Choi, Tanel Parnamaa, and Yoshua Bengio. A neural knowledge language model. *arXiv preprint arXiv:1608.00318*, 2016.

Mohammad Al Hasan and Mohammed J Zaki. A survey of link prediction in social networks. In *Social network data analytics*, pages 243–275. Springer, 2011.

Michael Ashburner, Catherine A. Ball, Judith A. Blake, David Botstein, Heather Butler, J. Michael Cherry, Allan P. Davis, Kara Dolinski, Selina S. Dwight, Janan T. Eppig, Midori A. Harris, David P. Hill, Laurie Issel-Tarver, Andrew Kasarskis, Suzanna Lewis, John C. Matese, Joel E. Richardson, Martin Ringwald, Gerald M. Rubin, and Gavin Sherlock. Gene Ontology: tool for the unification of biology. *Nat Genet*, 25(1):25–29, 2000.

J. Ba, K. Swersky, S. Fidler, and R. Salakhutdinov. Predicting deep zero-shot convolutional neural networks using textual descriptions. In *CVPR*, 2015.

Sean Bell and Kavita Bala. Learning visual similarity for product design with convolutional neural networks. *ACM Transactions on Graphics (TOG)*, 34(4):98, 2015.

Kurt Bollacker, Colin Evans, Praveen Paritosh, Tim Sturge, and Jamie Taylor. Freebase: A collaboratively created graph database for structuring human knowledge. In *SIGMOD*, pages 1247–1250, 2008.

Antoine Bordes, Nicolas Usunier, Alberto Garcia-Duran, Jason Weston, and Oksana Yakhnenko. Translating embeddings for modeling multi-relational data. In *Advances in Neural Information Processing Systems*, pages 2787–2795, 2013.

Li C., Lai Y., Goldwasser D., and Neville J. Joint embedding models for textual and social analysis. In *ICML Workshop*, 2017.

Xinlei Chen, Abhinav Shrivastava, and Abhinav Gupta. Neil: Extracting visual knowledge from web data. In *Proceedings of the IEEE International Conference on Computer Vision*, pages 1409–1416, 2013.

Abhishek Das, Satwik Kottur, Khushi Gupta, Avi Singh, Deshraj Yadav, Jose M. F. Moura, Devi Parikh, and Dhruv Batra. Visual dialog. In *CVPR*, July 2017.

J. Deng, W. Dong, R. Socher, L.-J. Li, K. Li, and L. Fei-Fei. ImageNet: A Large-Scale Hierarchical Image Database. In *CVPR*, 2009.

Carl Doersch, Abhinav Gupta, and Alexei A Efros. Mid-level visual element discovery as discriminative mode seeking. In *Advances in Neural Information Processing Systems 26*, pages 494–502. 2013.

Ali Farhadi, Ian Endres, Derek Hoiem, and David A. Forsyth. Describing objects by their attributes. In *2009 IEEE Computer Society Conference on Computer Vision and Pattern Recognition*, pages 1778–1785, 2009.

Pedro F Felzenszwalb, Ross B Girshick, David McAllester, and Deva Ramanan. Object detection with discriminatively trained part-based models. *IEEE transactions on pattern analysis and machine intelligence*, 32(9):1627–1645, 2010.

Matt Gardner and Tom M Mitchell. Efficient and expressive knowledge base completion using subgraph feature extraction. In *EMNLP*, pages 1488–1498, 2015.

Ross Girshick, Jeff Donahue, Trevor Darrell, and Jitendra Malik. Rich feature hierarchies for accurate object detection and semantic segmentation. In *Proceedings of CVPR*, pages 580–587, 2014.

Xavier Glorot and Yoshua Bengio. Understanding the difficulty of training deep feedforward neural networks. In *AISTATS*, 2010.

Abhinav Gupta, Aniruddha Kembhavi, and Larry S. Davis. Observing human-object interactions: Using spatial and functional compatibility for recognition. *IEEE Transactions on Pattern Analysis and Machine Intelligence*, 31:1775–1789, 2009.

Kelvin Guu, John Miller, and Percy Liang. Traversing knowledge graphs in vector space. *arXiv preprint arXiv:1506.01094*, 2015.

Ido Guy, Alexander Nus, Dan Pelleg, and Idan Szpektor. Care to share?: Learning to rank personal photos for public sharing. In *WSDM*, pages 207–215. ACM, 2018.

Hamid Izadinia, Fereshteh Sadeghi, and Ali Farhadi. Incorporating scene context and object layout into appearance modeling. In *Proceedings of the IEEE Conference on Computer Vision and Pattern Recognition*, pages 232–239, 2014.

Yangqing Jia, Evan Shelhamer, Jeff Donahue, Sergey Karayev, Jonathan Long, Ross Girshick, Sergio Guadarrama, and Trevor Darrell. Caffe: Convolutional architecture for fast feature embedding. *arXiv preprint arXiv:1408.5093*, 2014.

Lu Jiang, Yannis Kalantidis, Liangliang Cao, Sachin Farfade, Jiliang Tang, and Alexander G. Hauptmann. Delving deep into personal photo and video search. In *Proceedings of the Tenth ACM International Conference on Web Search and Data Mining*, WSDM, 2017.

J. Johnson, R. Krishna, M. Stark, L.-J. Li, D. A. Shamma, M. Bernstein, and L. Fei-Fei. Image retrieval using scene graphs. In *CVPR*, 2015.

Rudolf Kadlec, Ondrej Bajgar, and Jan Kleindienst. Knowledge base completion: Baselines strike back. *arXiv preprint arXiv:1705.10744*, 2017.

Ranjay Krishna, Yuke Zhu, Oliver Groth, Justin Johnson, Kenji Hata, Joshua Kravitz, Stephanie Chen, Yannis Kalantidis, Li-Jia Li, David A Shamma, Michael Bernstein, and Li Fei-Fei. Visual genome: Connecting language and vision using crowdsourced dense image annotations. In *arXiv preprint arXiv:1602.07332*, 2016.

Ni Lao, Tom Mitchell, and William W Cohen. Random walk inference and learning in a large scale knowledge base. In *Proceedings of the Conference on Empirical Methods in Natural Language Processing*, pages 529–539. Association for Computational Linguistics, 2011.

Yining Li, Chen Huang, Xiaoou Tang, and Chen Change Loy. Learning to disambiguate by asking discriminative questions. In *ICCV*, 2017.

Ziwei Liu, Ping Luo, Shi Qiu, Xiaogang Wang, and Xiaoou Tang. Deepfashion: Powering robust clothes recognition and retrieval with rich annotations. In *CVPR*, June 2016.

C. Lu, R. Krishna, M. Bernstein, and L. Fei-Fei. Visual relationship detection with language priors. In *ECCV*, 2016.

Tomasz Malisiewicz and Alexei A. Efros. Beyond categories: The visual memex model for reasoning about object relationships. In *Advances in Neural Information Processing Systems*, 2009.

Kenneth Marino, Ruslan Salakhutdinov, and Abhinav Gupta. The more you know: Using knowledge graphs for image classification. In *CVPR*, 2017.

Maximilian Nickel, Volker Tresp, and Hans-Peter Kriegel. A three-way model for collective learning on multi-relational data. In *Proceedings of the 28th international conference on machine learning (ICML-11)*, pages 809–816, 2011.

Maximilian Nickel, Kevin Murphy, Volker Tresp, and Evgeniy Gabrilovich. A review of relational machine learning for knowledge graphs. *Proceedings of the IEEE*, 104(1):11–33, 2016a.

Maximilian Nickel, Lorenzo Rosasco, and Tomaso A. Poggio. Holographic embeddings of knowledge graphs. In *Proceedings of the Thirtieth Conference on Artificial Intelligence*, pages 1955–1961, 2016b.

Wei Niu, James Caverlee, and Haokai Lu. Neural personalized ranking for image recommendation. In *Proceedings of the Eleventh ACM International Conference on Web Search and Data Mining*, WSDM, 2018.

Hyun Oh Song, Yu Xiang, Stefanie Jegelka, and Silvio Savarese. Deep metric learning via lifted structured feature embedding. In *Proceedings of the IEEE Conference on Computer Vision and Pattern Recognition*, pages 4004–4012, 2016.

Megha Pandey and Svetlana Lazebnik. Scene recognition and weakly supervised object localization with deformable part-based models. In *Computer Vision (ICCV), 2011 IEEE International Conference on*, pages 1307–1314, 2011.

Pouya Pezeshkpour, Liyan Chen, and Sameer Singh. Embedding multimodal relational data for knowledge base completion. In *EMNLP*, 2018.

B. Romera-Paredes and P. Torr. An embarrassingly simple approach to zero-shot learning. In *ICML*, 2015.

Olga Russakovsky, Jia Deng, Zhiheng Huang, Alexander C. Berg, and Li Fei-Fei. Detecting avocados to zucchinis: what have we done, and where are we going? In *International Conference on Computer Vision (ICCV)*, 2013.

Fereshteh Sadeghi and Marshall F. Tappen. Latent pyramidal regions for recognizing scenes. In *Proceedings of the 12th European Conference on Computer Vision - Volume Part V*, pages 228–241, 2012.

F. Schroff, D. Kalenichenko, and J. Philbin. Facenet: A unified embedding for face recognition and clustering. In *2015 IEEE Conference on Computer Vision and Pattern Recognition (CVPR)*, pages 815–823, 2015.

Iulian Vlad Serban, Alberto García-Durán, Caglar Gulcehre, Sungjin Ahn, Sarath Chandar, Aaron Courville, and Yoshua Bengio. Generating factoid questions with recurrent neural networks: The 30m factoid question-answer corpus. *arXiv preprint arXiv:1603.06807*, 2016.

K. Simonyan and A. Zisserman. Very deep convolutional networks for large-scale image recognition. *CoRR*, 2014.

Kihyuk Sohn. Improved deep metric learning with multi-class n-pair loss objective. In *Advances in Neural Information Processing Systems*, pages 1857–1865, 2016.

Hyun Oh Song, Stefanie Jegelka, Vivek Rathod, and Kevin Murphy. Deep metric learning via facility location. In *Conference on Computer Vision and Pattern Recognition (CVPR)*, 2017.

Damien Teney, Lingqiao Liu, and Anton van den Hengel. Graph-structured representations for visual question answering. In *CVPR*, July 2017.

Kristina Toutanova and Danqi Chen. Observed versus latent features for knowledge base and text inference. In *Proceedings of the 3rd Workshop on Continuous Vector Space Models and their Compositionality*, pages 57–66, 2015.

Rakshit Trivedi, Hanjun Dai, Yichen Wang, and Le Song. Know-evolve: Deep temporal reasoning for dynamic knowledge graphs. In *ICML*, 2017.

Théo Trouillon, Johannes Welbl, Sebastian Riedel, Éric Gaussier, and Guillaume Bouchard. Complex embeddings for simple link prediction. *arXiv preprint arXiv:1606.06357*, 2016.

Andreas Veit, Balazs Kovacs, Sean Bell, Julian McAuley, Kavita Bala, and Serge Belongie. Learning visual clothing style with heterogeneous dyadic co-occurrences. In *ICCV*, 2015.

Lonij Vincent, Rawat Ambrish, and Nicolae Maria-Irina. Extending knowledge bases using images. In *AKBC*, 2017.

Jian Wang, Feng Zhou, Shilei Wen, Xiao Liu, and Yuanqing Lin. Deep metric learning with angular loss. In *International Conference on Computer Vision (ICCV)*, 2017.

X. Wang, S. Qiu, K. Liu, and X. Tang. Web image re-ranking usingquery-specific semantic signatures. *IEEE Transactions on Pattern Analysis and Machine Intelligence*, 36(4): 810–823, April 2014.

David S. Wishart, Craig Knox, Anchi Guo, Dean Cheng, Savita Shrivastava, Dan Tzur, Bijaya Gautam, and Murtaza Hassanali. Drugbank: a knowledgebase for drugs, drug actions and drug targets. *Nucleic Acids Research*, 36:901–906, 2008.

Jianxiong Xiao, James Hays, Krista A. Ehinger, Aude Oliva, and Antonio Torralba. SUN database: Large-scale scene recognition from abbey to zoo. In *The Twenty-Third IEEE Conference on Computer Vision and Pattern Recognition*, pages 3485–3492, 2010.

Mohamed Yahya, Denilson Barbosa, Klaus Berberich, Qiuyue Wang, and Gerhard Weikum. Relationship queries on extended knowledge graphs. In *WSDM*, 2016.

Bishan Yang, Wen-tau Yih, Xiaodong He, Jianfeng Gao, and Li Deng. Learning multi-relational semantics using neural-embedding models. *arXiv preprint arXiv:1411.4072*, 2014.

X. Yang, T. Mei, Y. Zhang, J. Liu, and S. Satoh. Web image search re-ranking with click-based similarity and typicality. *IEEE Transactions on Image Processing*, 25(10): 4617–4630, 2016.

Bangpeng Yao and Li Fei-Fei. Modeling mutual context of object and human pose in human-object interaction activities. In *Computer Vision and Pattern Recognition (CVPR), 2010 IEEE Conference on*, pages 17–24, 2010.

Yuyu Zhang, Hanjun Dai, Zornitsa Kozareva, Alexander J. Smola, and Le Song. Variational reasoning for question answering with knowledge graph. In *AAAI*, 2018.

Z. Zhang and V. Saligrama. Zero-shot learning via semantic similarity embedding. In *ICCV*, 2015.

Feng Zhou and Yuanqing Lin. Fine-grained image classification by exploring bipartite-graph labels. In *CVPR*, June 2016.

Yuke Zhu, Alireza Fathi, and Li Fei-Fei. Reasoning about object affordances in a knowledge base representation. In *European conference on computer vision*, pages 408–424, 2014.